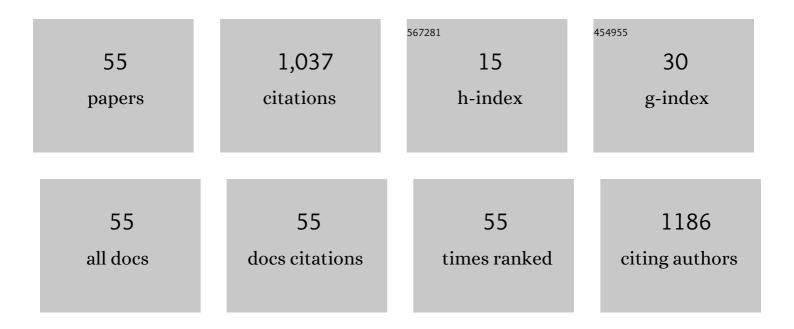
## Sebastian E Lauro

List of Publications by Year in descending order

Source: https://exaly.com/author-pdf/7103931/publications.pdf Version: 2024-02-01



#	Article	IF	CITATIONS
1	Radar evidence of subglacial liquid water on Mars. Science, 2018, 361, 490-493.	12.6	346
2	Multiple subglacial water bodies below the south pole of Mars unveiled by new MARSIS data. Nature Astronomy, 2021, 5, 63-70.	10.1	127
3	The Moon's farside shallow subsurface structure unveiled by Chang'E-4 Lunar Penetrating Radar. Science Advances, 2020, 6, eaay6898.	10.3	103
4	Dielectric properties of Jovian satellite ice analogs for subsurface radar exploration: A review. Reviews of Geophysics, 2015, 53, 593-641.	23.0	52
5	Pitfalls in GPR Data Interpretation: False Reflectors Detected in Lunar Radar Cross Sections by Chang'e-3. IEEE Transactions on Geoscience and Remote Sensing, 2018, 56, 1325-1335.	6.3	44
6	A controlled experiment to investigate the correlation between early-time signal attributes of ground-coupled radar and soil dielectric properties. Journal of Applied Geophysics, 2014, 101, 68-76.	2.1	35
7	GPR detectability of rocks in a Martian-like shallow subsoil: A numerical approach. Planetary and Space Science, 2012, 62, 31-40.	1.7	25
8	Analysis of GPR Early-Time Signal Features for the Evaluation of Soil Permittivity Through Numerical and Experimental Surveys. IEEE Journal of Selected Topics in Applied Earth Observations and Remote Sensing, 2016, 9, 178-187.	4.9	24
9	Dielectric constant estimation of the uppermost Basal Unit layer in the martian Boreales Scopuli region. Icarus, 2012, 219, 458-467.	2.5	23
10	Permittivity estimation of layers beneath the northern polar layered deposits, Mars. Geophysical Research Letters, 2010, 37, .	4.0	18
11	Estimation of subsurface dielectric target depth for GPR planetary exploration: Laboratory measurements and modeling. Journal of Applied Geophysics, 2013, 93, 93-100.	2.1	17
12	Radar Signal Penetration and Horizons Detection on Europa Through Numerical Simulations. IEEE Journal of Selected Topics in Applied Earth Observations and Remote Sensing, 2017, 10, 118-129.	4.9	17
13	Electromagnetic signal penetration in a planetary soil simulant: Estimated attenuation rates using CPR and TDR in volcanic deposits on Mount Etna. Journal of Geophysical Research E: Planets, 2017, 122, 1392-1404.	3.6	17
14	The Global Search for Liquid Water on Mars from Orbit: Current and Future Perspectives. Life, 2020, 10, 120.	2.4	16
15	Assessing the role of clay and salts on the origin of MARSIS basal bright reflections. Earth and Planetary Science Letters, 2022, 579, 117370.	4.4	15
16	GPR ESTIMATION OF THE GEOMETRICAL FEATURES OF BURIED METALLIC TARGETS IN TESTING CONDITIONS. Progress in Electromagnetics Research B, 2013, 49, 339-362.	1.0	14
17	Dielectric characterization of ice/MgSO 4 â‹11H 2 O mixtures as Jovian icy moon crust analogues. Earth and Planetary Science Letters, 2016, 439, 11-17.	4.4	13
18	Regional stratigraphy of the south polar layered deposits (Promethei Lingula, Mars): "Discontinuity-bounded―units in images and radargrams. Icarus, 2018, 308, 76-107.	2.5	11

SEBASTIAN E LAURO

#	Article	IF	CITATIONS
19	Radio wave techniques for non-destructive archaeological investigations. Contemporary Physics, 2011, 52, 121-130.	1.8	10
20	Stratigraphy versus artefacts in the Chang'e-4 low-frequency radar. Nature Astronomy, 2021, 5, 890-893.	10.1	10
21	Efficient Modeling of the Crosstalk Between Two Coupled Microstrip Lines Over Nonconventional Materials Using an Hybrid Technique. IEEE Transactions on Magnetics, 2008, 44, 1482-1485.	2.1	9
22	Symmetrical Coupled Microstrip Lines With Epsilon Negative Metamaterial Loading. IEEE Transactions on Magnetics, 2009, 45, 1182-1185.	2.1	9
23	GPR measurements and FDTD simulations for landmine detection. , 2010, , .		8
24	Coaxial-Cage Transmission Line for Electromagnetic Parameters Estimation. IEEE Transactions on Instrumentation and Measurement, 2013, 62, 2938-2942.	4.7	8
25	Survivability of Anhydrobiotic Cyanobacteria in Salty Ice: Implications for the Habitability of Icy Worlds. Life, 2019, 9, 86.	2.4	8
26	MAPPING THE UNDISCOVERED RUINS OF POMPEII (NAPLES, ITALY) USING GROUND PENETRATING RADAR*. Archaeometry, 2012, 54, 203-212.	1.3	7
27	Liquid Water Detection under the South Polar Layered Deposits of Mars—a Probabilistic Inversion Approach. Remote Sensing, 2019, 11, 2445.	4.0	7
28	Thermal and electromagnetic models for radar sounding of the galilean satellite icy crusts. , 2014, , .		6
29	Groundâ€penetrating Radar in the <i>Regio III</i> (Pompeii, Italy): Archaeological Evidence. Archaeological Prospection, 2011, 18, 187-194.	2.2	5
30	An evaluation of the early-time GPR amplitude technique for electrical conductivity monitoring. , 2013, , .		5
31	A critical analysis on the uncertainty computation in ground-penetrating radar-retrieved dry snow parameters. Geophysics, 2020, 85, H39-H49.	2.6	4
32	Loss tangent estimation from ground-penetrating radar data using Ricker wavelet centroid-frequency shift analysis. Geophysics, 2022, 87, H1-H12.	2.6	4
33	Dry snow permittivity evaluation from density: A critical review. , 2018, , .		3
34	"Unconformity-Bounded―Stratigraphic Units in the South Polar Layered Deposits (Promethei Lingula,) Tj ET	QqQ 9 0 r	gBŢ /Overlock
35	Coupled microstriplines with ENG metamaterial loading: physical concepts, design formulas, and numerical simulations 2007		2

36 Shape reconstruction of scatterers by suitable inverse processing of GPR data. , 2012, , .

2

#	Article	IF	CITATIONS
37	Numerical and experimental surveys on the GPR early-time signal features for the evaluation of shallow-soil permittivity. , 2014, , .		2
38	Accurate analysis of GPR first-arrival signals for the evaluation of soil permittivity parameters. , 2015, , .		2
39	Combined GPR and TDR measurements for snow thickness and density estimation. , 2015, , .		2
40	Metamaterials as complex dielectrics in the design of a new class of integrated circuits. , 2007, , .		1
41	Ground-Penetrating Radar technique to investigate historic eruptions on the Mt. Etna volcano (Sicily,) Tj ETQq1	1 0.784314	ŀrgBT /Overl
42	Electromagnetic parameters measurements of clay soils for Mars radar sounding. , 2014, , .		1
43	Young sea ice electric properties estimation under non-optimal conditions. , 2017, , .		1
44	Enhanced coupling values in coupled microstriplines using metamaterials. , 2007, , .		0
45	Analysis of polarizing properties of Birefringent Negative Indexed Materials at optical frequencies. , 2008, , .		0
46	BEM analysis of electromagnetic components filled with unconventional materials. COMPEL - the International Journal for Computation and Mathematics in Electrical and Electronic Engineering, 2008, 27, 1273-1285.	0.9	0
47	GPR characterization of rocks buried in the Martian subsoil. , 2010, , .		0
48	A simple inversion model for the estimation of subsurface features of Mars poles. , 2010, , .		0
49	Development of an efficient numerical set-up to predict the performance of ground-penetrating-radar systems for on-site Earth and planetary applications. , 2011, , .		0
50	Dielectric measurements of saline ices: Implications for jovian satellites radar exploration. , 2011, , .		0
51	Electromagnetic characterization of saline mixture for shallow radar exploration. , 2014, , .		0
52	Volume Scattering Losses Evaluation for Radar Sounding of Jovian Icy Moons. , 2018, , .		0
53	Dielectric Characterization of Ice/Na <inf>2</inf> SO <inf>4</inf> ·10H <inf>2</inf> O Mixtures: Implications for Radar Investigations of Icy Satellites. , 2018, , .		0
54	Radar detection of subglacial water under the south polar cap of Mars: Where are we now?. , 2020, , .		0

#	Article	IF	CITATIONS
55	Combining active seismic data from Apollo 14 and 16 with ground penetrating radar results to examine the shallow lunar subsurface. Planetary and Space Science, 2022, 214, 105460.	1.7	Ο